

# Cyclodextrin-Modified Zeolites: Host–Guest Surface Chemistry for the Construction of Multifunctional Nanocontainers

Anna Szarpak-Jankowska,<sup>[a]</sup> Christine Burgess,<sup>[a, b, c]</sup> Luisa De Cola,<sup>\*[a, b, c]</sup> and Jurriaan Huskens<sup>\*[a]</sup>

**Abstract:** The functionalization of nanoporous zeolite L crystals with  $\beta$ -cyclodextrin (CD) has been demonstrated. The zeolite surface was first modified with amino groups by using two different aminoalkoxysilanes. Then, 1,4-phenylene diisothiocyanate was reacted with the amino monolayer and used to bind CD heptamine by using its remaining isothiocyanate groups. The use of the different aminoalkoxysilanes, 3-aminopropyl dimethylmethoxysilane (APDMES) and 3-aminopropyl triethoxysilane (APTES), led

to drastic differences in uptake and release properties. Thionine was found to be absorbed and released from amino- and CD-functionalized zeolites when APDMES was used, whereas functionalization by APTES led to complete blockage of the zeolite channels. Fluorescence microscopy showed that the CD groups covalently attached to the

zeolite crystals could bind adamantyl-modified dyes in a specific and reversible manner. This strategy allowed the specific immobilization of His-tagged proteins by using combined host–guest and His-tag-Ni-nitrilotriacetic acid (NTA) coordination chemistry. Such multifunctional systems have the potential for encapsulation of drug molecules inside the zeolite pores and non-covalent attachment of other (for example, targeting) ligand molecules on its surface.

**Keywords:** cyclodextrins • host–guest systems • nanocontainers • proteins • zeolites

## Introduction

Multifunctional nanocontainers for imaging, targeting, and drug release are nowadays a main research area in bio-nanomedicine.<sup>[1]</sup> A nanocontainer should act as a carrier for therapeutics and imaging agents, deliver its payload to the specific target, and release its content at the desired moment with preserved activity. Such a nanostructure should be carefully designed with suitable functionalities useful for detection, recognition, and treatment. Inorganic porous materials such as colloidal silica and various aluminosilicates are attractive owing to their high loading efficiency and shielding capability of bioactive molecules.<sup>[2]</sup>

Zeolites are transparent, robust aluminosilicates synthesized in the micro/nano size range, based on a framework of  $\text{SiO}_4$  and  $\text{AlO}_4$  tetrahedrons resulting in pores and channels capable of encapsulating small molecules. Besides the use of zeolites in industrial, environmental, and biotechnological applications, they have emerged as potential candidates for medical applications such as skin wound healing, bone formation, and hemodialysis.<sup>[3]</sup> Several types of zeolites have been studied for drug release such as zeolite Y as a carrier of anthelmintic drugs,<sup>[4]</sup> zeolite X for the absorption and release of ketoprofen,<sup>[5]</sup> and a CuX zeolite as a support for cyclophosphamide in antitumor therapy.<sup>[6]</sup> Recently, zeolite/polymer composite hollow microspheres with a prolonged antibiotic release were demonstrated.<sup>[7]</sup> In all of these cases, the drugs are enclosed in the pores of the zeolite crystals to be released at a desired moment in a suitable environment.

Zeolite L is an aluminosilicate composed of unidirectional channels possessing entrance diameters of 0.71 nm. Depending on the synthesis conditions, the length of the crystals can be varied from 30 nm up to about 10  $\mu\text{m}$ .<sup>[8]</sup> The form and aspect ratio can also be tuned allowing the production of materials with nanosized, disc, or cylindrical shape. Owing to the presence of Al, the framework is negatively charged, which endows the zeolites with cation-exchange capabilities, thus allowing the uptake and release of charged molecules.<sup>[9]</sup> Some studies concern the surface modification of zeolite L for the attachment of  $\text{Gd}^{\text{III}}$ - and  $\text{Eu}^{\text{III}}$ -DOTA (1,4,7,10-tetraazacyclododecane-1,4,7,10-tetraacetic acid) complexes for MRI imaging,<sup>[10]</sup> an arginylglycylaspartic (RGD) peptide for cell adhesion,<sup>[11]</sup> or spiropyran for biosensing.<sup>[12]</sup> However, to

[a] Dr. A. Szarpak-Jankowska, Dr. C. Burgess, Prof. L. De Cola, Prof. Dr. J. Huskens  
Molecular Nanofabrication Group  
MESA + Institute for Nanotechnology, University of Twente  
P.O. Box 217, 7500 AE Enschede (The Netherlands)  
Fax: (+31) 53-4894645  
E-mail: decola@unistra.fr  
j.huskens@utwente.nl

[b] Dr. C. Burgess, Prof. L. De Cola  
Westfälische Wilhelms-Universität Münster  
Mendelstrasse 7, 48149 Münster (Germany)

[c] Dr. C. Burgess, Prof. L. De Cola  
Current address:  
Institut de Science et d'Ingénierie Supramoléculaires  
Université de Strasbourg, 8 allée Gaspard Monge  
67000 Strasbourg (France)

Supporting information for this article is available on the WWW under <http://dx.doi.org/10.1002/chem.201302153>.

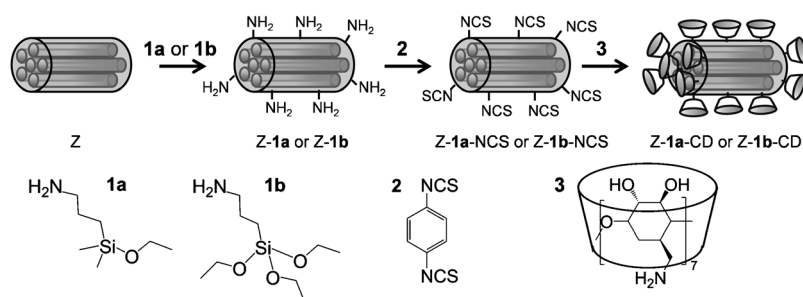
address the suitability of zeolite L as a potential drug carrier, functionalization of its outer surface needs to be studied congruently with its uptake and release properties as the former may influence the latter.

In this study, we present the use of cyclodextrin (CD) host-guest chemistry as a model system for covalent and noncovalent functionalization of the zeolite surface. We study the release properties as a function of the covalent monolayer structure and show that the noncovalent host-guest chemistry can be used to bind molecules and proteins to the covalent receptor-functionalized outer surface of the zeolite.

## Results and Discussion

**Surface functionalization of zeolite L and its influence on uptake and release:** The procedure for the preparation of the CD-functionalized zeolite L is shown in Scheme 1. The first step of the reaction involves employing alkoxysilanes that are known to react with free Si-OH groups on the zeolite surface (Z). Multifunctional alkoxysilanes (for example, trichloro or trialkoxy derivatives) bind to the surface but simultaneously form covalent bonds between adjacent molecules, a fact that can lead to polymerization and may limit the permeability of the formed layer.<sup>[13]</sup> Therefore, two different aminosilanes, APDMES (**1a**) with one ethoxy group and APTES (**1b**) with three ethoxy groups, were studied. Amino-terminated zeolite L (Z-**1a** or Z-**1b**) was reacted in the next step with *p*-phenylene diisothiocyanate (DITC, **2**) to transform the amino surface to free isothiocyanate groups.<sup>[14]</sup> In the next step, CD heptamine (**3**) was bound to the isothiocyanate groups, yielding CD-terminated zeolite L (Z-**1a**-CD or Z-**1b**-CD).

X-ray photoelectron spectroscopy (XPS) was used to determine the surface composition after modification of the zeolite. The high-resolution N<sub>1s</sub> scans for the crystals functionalized with APDMES (**1a**), APTES (**1b**), and the resulting Z-CD products are given in Figure 1 a. Apart from the unmodified zeolite (Z), all elemental scans showed a N<sub>1s</sub> peak at approximately 398 eV. Moreover, in the spectra of Z-CD, we observed a sulfur peak (S<sub>2p</sub> at approximately 161 eV, Figure 1 b), which arose upon activation with **2**. The



Scheme 1. Schematic representation of zeolite L functionalization: native (Z), amino-functionalized (Z-**1a** or Z-**1b**), NCS-functionalized (Z-**1a**-NCS or Z-**1b**-NCS), and  $\beta$ -cyclodextrin (CD)-modified (Z-**1a**-CD or Z-**1b**-CD) zeolite L.

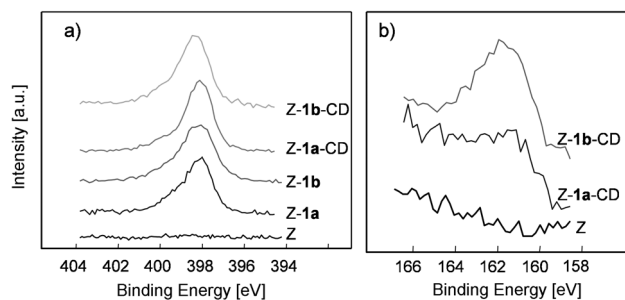


Figure 1. High-resolution XPS spectra: a) N<sub>1s</sub> spectra of Z, Z-**1a**, Z-**1b**, Z-**1a**-CD, and Z-**1b**-CD; b) S<sub>2p</sub> spectra of Z, Z-**1a**-CD, and Z-**1b**-CD.

carbon-to-nitrogen (C/N) atomic ratio increased from 4.2 and 5.5 in Z-NH<sub>2</sub> to 8.5 and 8.05 for Z-CD when using **1a** and **1b**, respectively. The increase of the C/N ratio after the last step of functionalization provides further evidence for the attachment of CD heptamine. The similar C/N values for zeolites modified with **1a** and **1b** indicate that the density of amino groups in both cases is comparable.

Zeta-potential measurements of native and CD-modified zeolites showed an increase from  $-59.5$  mV for Z to  $+31.4$  and  $+42.2$  mV for Z-**1a**-CD and Z-**1b**-CD, respectively. As shown before on flat substrates,<sup>[15]</sup> not all amino groups of CD heptamine are involved in the formation of covalent bonds upon attachment to NCS-covered surfaces, thus the presence of free and charged (protonated) amino groups on the CD units results in a positive zeta-potential value.

To mimic the encapsulation of small drug molecules, we selected the fluorescent dye thionine (Figure 2 a). Thionine is a fluorescent molecule that can be incorporated into the channels of zeolite L by cation exchange, replacing the accessible counterions of the zeolite framework. The loading of native zeolite L with thionine fluorescent molecules has been reported before.<sup>[10,16]</sup> Here, we studied the effect of zeolite surface functionalization on the uptake and release of thionine.

First, we compared the uptake of thionine by native, amino- and CD-functionalized zeolites. For the amino functionalization, we have also investigated the role played by the anchoring silane groups by comparing the derivatives **1a** and **1b**. Suspensions of individual zeolite samples in thionine solutions ( $10 \mu\text{M}$ ) were stirred for 4 h. The thionine cations exposed to zeolite L can also be physisorbed on the external surface of the crystal. To remove the physisorbed material, the samples were washed with large amounts of EtOH and an aqueous solution of tetrabutylammonium chloride (TBACl). The tetrabutylammonium cation is a large bulky cation that can remove electrostatically attached ions only from the surface, as it cannot penetrate the zeolite channels.

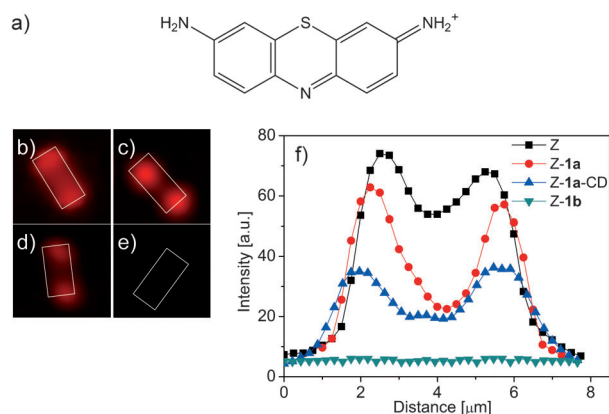


Figure 2. a) Structure of thionine. b–e) Fluorescence microscopy images of thionine-loaded zeolites: Z (b), Z-1a (c), Z-1a-CD (d), Z-1b (e). f) Corresponding fluorescence intensity profiles along the zeolite crystals.

To be sure that all thionine molecules were removed from the crystal surface, the supernatant was analyzed using UV/Vis spectroscopy and rinsing was continued until the supernatant was free of thionine. The fluorescence images of the zeolites are shown in Figure 2. We observed the presence of the thionine dye inside of Z, Z-1a, and Z-1a-CD (Figure 2b–d). The fluorescence intensity was found to be stronger for the native zeolite, whereas it was somewhat weaker in the functionalized crystals. Surprisingly, no fluorescence was detected in Z-1b when APTES was used for modification (Figure 2e).

Owing to the very long channels in the 4 μm zeolite L, the loading with thionine cannot be completely uniform. Indeed, a higher concentration of the dye molecules is observed at the channel entrances and a lower concentration is expected in the middle of the crystal. Ions penetrate the cylindrical pores from both sides along the direction of the cylinder axis.<sup>[17]</sup> In Z-1a and Z-1a-CD, entrapment of the dyes was approximately 20 or 50% less, respectively, estimated from a single zeolite emission intensity, compared with the native zeolite. The absence of fluorescence in Z-1b indicates a lack of uptake of dye in this case. Closing of the pores has probably occurred, an observation that is attributed to APTES (1b) forming a mono- or multilayer film with many interconnecting bonds owing to the presence of the three reactive silane groups.<sup>[13]</sup> In contrast, APDMES (1a), with two inert methyl and only one reactive ethoxy group, is attached to the surface of the zeolite by one silanol bond only and does not allow additional bond formation with adjacent molecules. Apparently, this leaves the pores of Z-1a and Z-1a-CD accessible for cation exchange.

To study the release of thionine from the modified zeolites, the dye was first loaded in the native zeolite L by ion exchange, followed by functionalization of the crystals with amino and CD groups according to Scheme 1, and finally by dispersion of the crystals in 0.15 M NaCl, in which thionine should be liberated by exchange with Na<sup>+</sup>. The concentration of released dye was monitored by UV/Vis spectroscopy (Figure 3). Figure 3 demonstrates that thionine can be re-

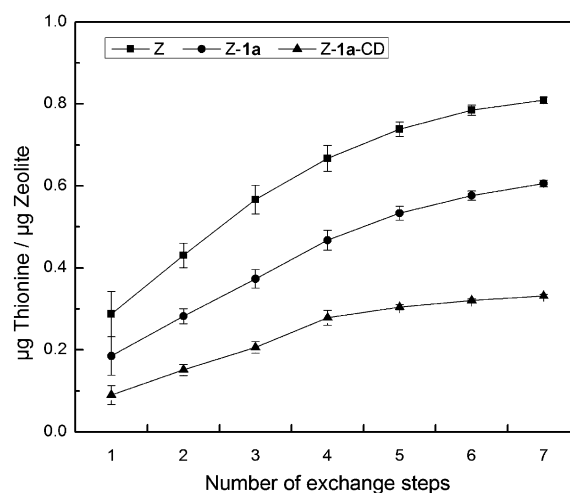


Figure 3. Cumulative amounts of thionine dye released from native Z (squares), Z-1a (circles), and Z-1a-CD (triangles) as a function of the step number in the exchange process. Each step was performed by using a fresh portion of 0.15 M NaCl for 2 h.

leased from the channels of amino- and CD-surface-functionalized zeolites when APDMES (1a) was used for functionalization. The amounts of thionine released from the Z-1a and Z-1a-CD crystals during the first 2 h, or after all release steps, were about 30% and 70% lower than from the native zeolite, respectively. After four to five redispersions in fresh aqueous NaCl, the amount of additionally released thionine became very small. A similar experiment performed on amino-zeolite L modified with APTES (1b) showed an insignificant amount (7-fold lower than when modified with APDMES) of released thionine during the first 2 h (data not shown). The differences in release rates are comparable to the differences observed during uptake (see above), and reflect the same effect of monolayer properties on the cation exchange process. These results indicate that a rather large molecule can be trapped inside the zeolite particle indefinitely when using APTES, which could be useful, for example, for imaging purposes, whereas functionalization with APDMES allows reversible uptake and release, which is suited for drug carrier purposes. In all subsequent experiments, only 1a was used as the amino linker.

**Functionalization of zeolites by surface host-guest chemistry:** Adamantyl-modified fluorescent dyes were selected to study host-guest interactions with the CD-functionalized zeolites. The water-soluble fluorescein-Ad<sub>2</sub> molecule (Figure 4a) is known to interact with CD cavities immobilized onto a surface by using its Ad moieties to form a strong noncovalent complex (with a binding constant of  $\sim 10^{10} \text{ M}^{-1}$ ).<sup>[18]</sup>

Z-1a-CD crystals were suspended in a 1 μM aqueous solution of fluorescein-Ad<sub>2</sub> (in phosphate buffered saline, PBS, pH 7.4) and sonicated for 1 min. Removal of excess and physisorbed dye was performed by centrifugation as well as redispersion of the zeolite crystals in PBS buffer (three times). As a reference experiment, adsorption of the diva-

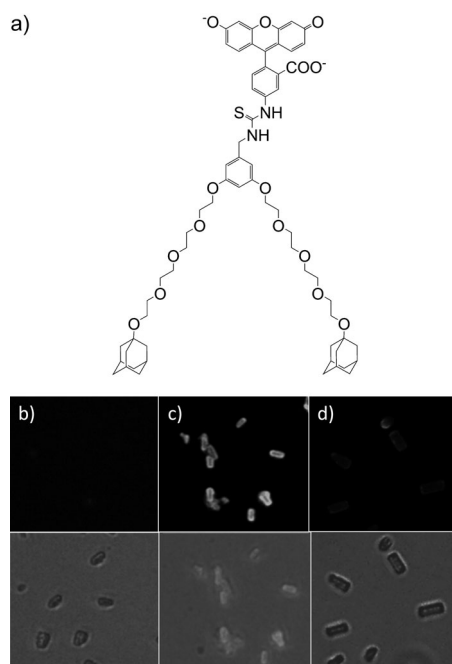


Figure 4. a) Structure of fluorescein-Ad<sub>2</sub>. b–d) Fluorescence (top) and optical (bottom) microscopy images of **Z-1a** (b) and **Z-1a-CD** (c) after adsorption of fluorescein-Ad<sub>2</sub> and triple rinsing with PBS, and **Z-1a-CD** (d) after subsequent desorption of dye in 10 mM aqueous CD.

lent dye onto **Z-1a** was performed under the same conditions. An intense fluorescence was observed (Figure 4c) for **Z-1a-CD**. In contrast, negligible emission was observed for **Z-1a** (Figure 4b). These results confirm that the dye molecules are bound selectively by the CD cavities by specific host–guest interactions.

Next, the **Z-1a-CD** crystals with adsorbed fluorescein-Ad<sub>2</sub> were sonicated in CD and PBS (as a control) solutions. After 30 min, we observed a negligible loss of dye in PBS while almost full desorption occurred in the CD solution (Figure 4d). When bound fluorescein-Ad<sub>2</sub> is exposed to a solution of CD, competition is induced between binding of the dye's guest groups to the surface CD sites and the CD in solution, resulting in desorption of the fluorescent guest, similar to previous observations on planar substrates.<sup>[15]</sup>

When **Z-1a-CD** was exposed to a solution of dye molecules equipped with only one adamantyl moiety, the fluorescence intensity after triple rinsing with PBS was much lower than for the divalent lissamine-Ad<sub>2</sub> (see the Supporting Information, Figures S1 and S2). The binding constant of a single adamantyl unit to a surface with immobilized CD is only  $4.6 \times 10^4 \text{ M}^{-1}$ , which is much lower than the binding strength of a molecule bearing two adamantyl groups (approx.  $10^{10} \text{ M}^{-1}$ ),<sup>[19]</sup> causing facile desorption from the CD cavities in the monovalent case. These results show that a multivalent guest binds significantly stronger to the CD-functionalized zeolite surface. This indicates that the CD coverage on the zeolite surface must be relatively high as two Ad groups grafted on one dye molecule can interact

with two CD moieties on the zeolite surface only if the two cavities are close enough.

As a proof of concept that the zeolites can be loaded and surface-functionalized in an orthogonal manner (that is, without mutual interference), CD-functionalized zeolite L (**Z-1a-CD**) internally loaded with thionine was exposed to a solution of fluorescein-Ad<sub>2</sub>. A fluorescence microscopy image of the resulting zeolites is presented in Figure 5c. The

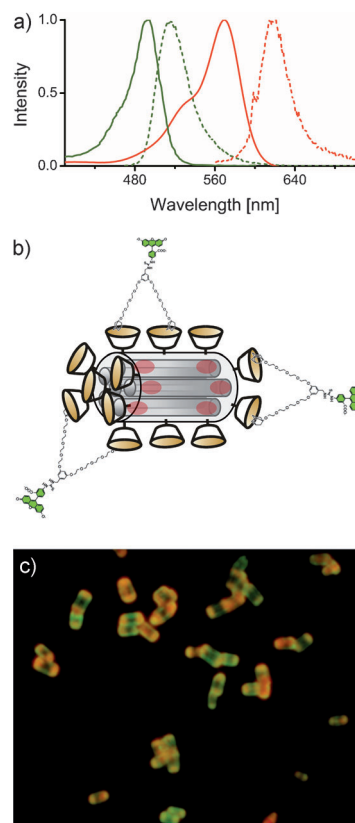
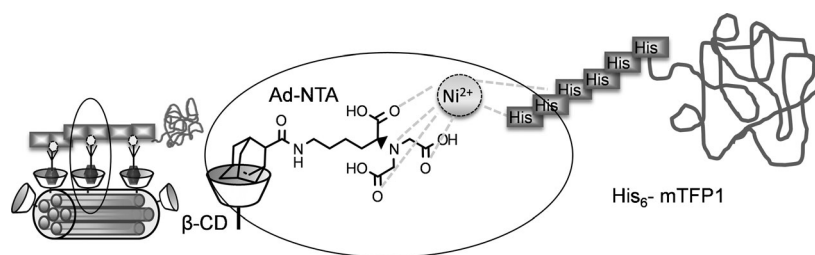


Figure 5. a) Excitation (solid) and emission (dashed) spectra for fluorescein-Ad<sub>2</sub> (green) and thionine (red). b) Cartoon of **Z-1a-CD** with thionine in the interior and fluorescein-Ad<sub>2</sub> noncovalently bound to the outside. c) Fluorescence image of **Z-1a-CD** ( $\lambda_{\text{exc}} = 450\text{--}480 \text{ nm}$ ,  $\lambda_{\text{em}} > 515 \text{ nm}$ ).

zeolites hosting two dyes were excited at  $\lambda = 450\text{--}480 \text{ nm}$  and observed at  $\lambda > 515 \text{ nm}$ . These settings allow both the simultaneous excitation and observation of both dyes (Figure 5a). As thionine is concentrated at the channel entrances whereas fluorescein covers the whole external surface of the zeolites (Figure 5b), the terminal parts of the crystals show a mixture of both colors while the central parts of the zeolites exhibit only the green fluorescein emission. The internal absorption of (drug) molecules and outer functionalization of **Z-1a-CD** with targeting vectors could make this orthogonal strategy, using CD-functionalized zeolite L, attractive for application as a controlled drug delivery system.

To demonstrate the possibility of functionalization with target-specific agents, ligands, or nanoparticles, we investi-

gated the attachment of a His-tagged protein as a model system. We used the visible teal fluorescent protein (TFP), which acts directly as an indicator of the bound protein on the surface without the need of any additional labeling steps for visualization. We employed the His<sub>6</sub> tag for binding the protein to the zeolite surface; the His<sub>6</sub> tag was designed into TFP for purification purposes by using its well-known affinity for Ni-nitrilotriacetate (NiNTA) complexes. To attach the His<sub>6</sub>-TFP to the Z-1a-CD, adamantyl-modified NTA (Ad-NTA) was used as an intermediate linker (Scheme 2).<sup>[20]</sup> Crystals of Z-1a-CD were incubated in three different solutions: (i) His<sub>6</sub>-TFP only; (ii) His<sub>6</sub>-TFP and Ad-NTA; (iii) His<sub>6</sub>-TFP, Ni<sup>2+</sup>, and Ad-NTA. Optical and fluorescence



Scheme 2. Binding of His<sub>6</sub>-TFP through Ni<sup>2+</sup>/Ad-NTA to CD immobilized on the zeolite surface.

images and fluorescence intensity profiles, obtained after 20 min of adsorption followed by rinsing five times, are shown in Figure 6. By far the highest intensity was observed when both the Ad-NTA linker and Ni<sup>2+</sup> were present in the solution. This confirms the specific binding of the protein through combined host-guest (CD-Ad) and metal-ligand (His<sub>6</sub>-NiNTA) coordination interactions. The same experiment repeated with much lower concentrations of protein (1.3 μM) showed a similarly high fluorescence intensity (data not shown) indicating that specific interactions promote easy attachment onto the surface.

In conclusion, we have shown the successful functionalization of zeolite L with cyclodextrins. Two different aminosilanes, APDMES and APTES, were used for surface modification. However, they showed a pronouncedly different effect on the accessibility of the channels of the zeolites for cation exchange. APTES formed an impermeable layer and blocked the diffusion of thionine dye molecules inside the crystals practically completely, whereas APDMES allowed exchange of the K<sup>+</sup> ions with the charged dye molecules, albeit to a lower extent than unmodified zeolite. By using this approach, ions can be trapped inside the channels permanently by using APTES (potentially useful for imaging) or can be released from amino- and CD-modified zeolites if the monovalent APDMES is used (potentially useful for drug delivery).

We have demonstrated that CD-modified zeolite L can play the role of a “double host” for drug molecules inside the pores and other molecules (for example, for targeting) attached to its surface. The CD-functionalized zeolites showed the reversible attachment of adamantyl-modified dyes and the specific immobilization of His-tagged proteins through combined His-tag-NiNTA and CD-Ad interactions. Our multifunctional system provides perspectives for the attachment of peptides or antibodies for specific targeting.

In conclusion, the supramolecular functionalization of the zeolite surface allows the immobilization of different molecules and biomolecules required for the construction of a multifunctional drug delivery system.

## Experimental Section

β-Cyclodextrin (CD) heptamine and fluorescent dyes modified with adamantyl (Ad) groups, such as fluorescein-Ad<sub>2</sub>, lissamine-Ad<sub>2</sub>, lissamine-Ad, and Ad-NTA, were synthesized according to previously published procedures.<sup>[15,18,20,21]</sup> Thionine was purchased from Sigma-Aldrich, 3-aminopropyl triethoxysilane (APTES), (3-aminopropyl) dimethylthoxysilane (APDMES), and *p*-phenylene diisothiocyanate (DITC) were obtained from Acros. The sequence encoding for the His<sub>6</sub>-TFP protein was purchased from Allele Biotechnology & Pharmaceuticals. The His<sub>6</sub>-TFP is an engineered variant of *Clavularia sp.* fluorescent protein cFP484. The sequence was

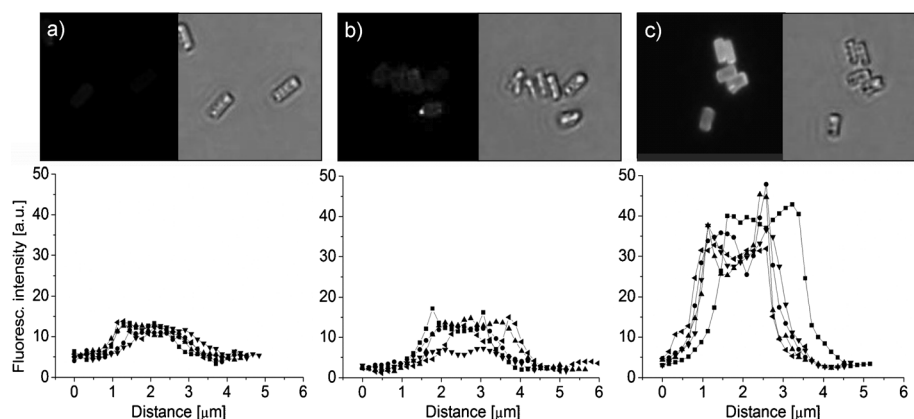


Figure 6. Simultaneous optical (right) and fluorescence (left) images, and the corresponding intensity profiles (bottom), of Z-1a-CD after incubation in solutions of a) His<sub>6</sub>-TFP (20 μM) only, b) His<sub>6</sub>-TFP (20 μM) and Ad-NTA (100 μM), and c) His<sub>6</sub>-TFP (20 μM) and Ni<sup>2+</sup>-Ad-NTA (100 μM).



cloned into a pET15 vector and expressed in *E. Coli* BL (DE3) pLysS (Novagen) and purified by using the standard Novagen His-bind protocol. Milli-Q water with a resistivity higher than 18 MWcm was used in all experiments.

**Preparation of zeolite L:** Zeolite L (4  $\mu\text{m}$ , Z) was synthesized according to a procedure described before.<sup>[8]</sup> In short, potassium hydroxide, sodium hydroxide, and aluminum hydroxide were diluted in distilled water, followed by the addition of a silica suspension and vigorous stirring of the mixture. The obtained gel was kept in an oven for 144 h at 160°C. The obtained white solid underwent ion exchange with 0.1 M KNO<sub>3</sub>, washed with water, and dried.

**Functionalization of zeolite L:** Amino-modified zeolite L crystals were prepared according to the slightly modified procedure of Tsotsalas et al.<sup>[10]</sup> Zeolite L crystals (100 mg) were dispersed in toluene (10 mL) followed by the addition of 100  $\mu\text{L}$  of APDMES (**1a**) or APTES (**1b**) and sonication for 2 h. The excess unreacted alkoxy silane was removed by centrifugation with toluene (two times) and EtOH (three times). In the next step, amino-terminated zeolite L crystals (**Z-1a** or **Z-1b**) were redispersed in DITC (0.05 M) in EtOH for 2 h at 40°C. The washed (EtOH, three times, centrifugation) DITC-functionalized crystals (**Z-1a-NCS** or **Z-1b-NCS**) were subsequently redispersed in an aqueous solution of the CD heptamine (0.4 M) and the reaction took place over 2 h (40°C). Finally, the CD-modified zeolite L (**Z-1a-CD** or **Z-1b-CD**) crystals were washed with water (five times).

**Binding of Ad-modified dyes to the surface of CD-functionalized zeolite L:** **Z-1a-CD** or **Z-1b-CD** (0.5 mg) was dispersed in 1 mL of a solution of the mono- or divalent Ad-modified dye (1  $\mu\text{M}$  of Ad moieties) in PBS buffer (pH 7.4) and subjected to sonication for 1 min. The excess of dye was removed by centrifugation. Any physisorbed dye was removed subsequently by washing with PBS buffer (three times). Fluorescence values were calculated from measurements of 7–10 zeolites.

**Protein attachment to CD-functionalized zeolite L:** Three solutions of protein His<sub>6</sub>-TFP in PBS buffer were prepared (in the presence of 1 mM Tween 20 to avoid nonspecific adsorption of protein): i) His<sub>6</sub>-TFP (20  $\mu\text{M}$ ); ii) His<sub>6</sub>-TFP (20  $\mu\text{M}$ ) mixed with Ad-NTA (100  $\mu\text{M}$ ); iii) His<sub>6</sub>-TFP (20  $\mu\text{M}$ ) mixed with Ad-NTA (100  $\mu\text{M}$ ) and NiCl<sub>2</sub> (100  $\mu\text{M}$ ). Samples containing 1 mg of zeolite crystals (**Z-1a-CD** or **Z-1b-CD**) were agitated in i), ii), or iii) for 20 min. Nonspecifically adsorbed material was removed by washing with PBS buffer with surfactant (five times) and the crystals were observed by using a fluorescence microscope.

**Loading and release:** A weighed amount of dried zeolite L was added to an aqueous solution of thionine (10  $\mu\text{M}$ ). Cation exchange was achieved upon heating to 70°C overnight, under vigorous stirring. To remove free dye adsorbed on the crystal surface, the zeolite crystals were dispersed in EtOH, sonicated for 10 s, and centrifuged. The supernatant was removed and a new portion (15 mL) of EtOH was added. The washing step with EtOH was repeated ten times, followed by washing with an aqueous solution of TBACl (0.1 M, five times).

For the release study, thionine-loaded zeolites (native or functionalized) were dispersed in an aqueous solution of NaCl (0.15 M) and sonicated at 25°C. The amount of released thionine was measured from the supernatant taken from the sample after separation by centrifugation (5 min, 7000 rpm). After 2 h of sonication and supernatant removal, a new portion of NaCl was added and the process was repeated. The amount of released dye was determined by UV/Vis absorption spectroscopy using extinction coefficient of  $0.53 \times 10^5 \text{ M}^{-1} \text{ cm}^{-1}$ .<sup>[16]</sup>

**Fluorescence microscopy:** Fluorescence microscopy images were taken using an Olympus inverted research microscope iX71 equipped with a mercury burner U-RFL-T as light source and an Olympus DP70 digital camera for image acquisition. Blue excitation light ( $450 \leq \lambda \leq 480 \text{ nm}$ ) and green emission light ( $\lambda \leq 515 \text{ nm}$ ) was filtered by using a U-MWB Olympus filter cube. Green excitation ( $510 \leq \lambda \leq 550 \text{ nm}$ ) and red emission light ( $\lambda \geq 590 \text{ nm}$ ) was filtered using a U-MWG Olympus filter cube.

**XPS measurements:** These were performed on a Quanterra Scanning X-ray Multiprobe instrument from Physical Electronics, equipped with a monochromatic Al<sub>K $\alpha$</sub>  X-ray source producing approximately 25 W of X-ray power.

**Zeta-potential measurements:** Zeta potentials of native and modified zeolites were measured by using a Malvern Zetasizer NanoZS. All measurements were performed at 25°C, in a solution of 0.01 M NaCl, pH 7. The zeta potential was calculated from the electrophoretic mobility ( $\mu$ ) by using the Smoluchowski function  $\zeta = \mu \eta / \epsilon$ , where  $\eta$  and  $\epsilon$  are the viscosity and permittivity of the solvent, respectively.

## Acknowledgements

The research leading to these results has received funding from the European Community's Seventh Framework Programme under grant agreement number CP-FP 228622–2 MAGNIFYCO. We are grateful to Gerard Kip for XPS analysis, Jordi Cabanas Danés for Ad-NTA synthesis, and Rik Rurup for providing mTGP1.

- [1] a) X. Xue, F. Wang, X. Liu, *J. Mater. Chem.* **2011**, *21*, 13107; b) M. E. Gindy, R. K. Prud'homme, *Expert Opin. Drug Delivery* **2009**, *6*, 865.
- [2] K. K. Cotí, M. E. Belowich, M. Liong, M. W. Ambrogio, Y. A. Lau, H. A. Khatib, J. I. Zink, N. M. Khashab, J. F. Stoddart, *Nanoscale* **2009**, *1*, 16.
- [3] S. M. Auerbach, K. A. Carrado, P. K. Dutta, *Handbook of Zeolite Science and Technology*, Marcel Dekker, New York, **2003**.
- [4] A. Dyer, S. Morgan, P. Wells, C. Williams, *J. Helminthol.* **2000**, *74*, 137.
- [5] M. G. Rimoli, M. R. Rabaioli, D. Melisi, A. Curcio, S. Mondello, R. Mirabelli, E. Abignente, *J. Biomed. Mater. Res. Part A* **2008**, *87A*, 156.
- [6] C. V. Uglea, I. Albu, A. Vatajanu, M. Croitoru, S. Antoniu, L. Panaitescu, R. M. Ottenbrite, *J. Biomater. Sci. Polym. Ed.* **1995**, *6*, 633.
- [7] X. C. Zhang, Y. He, Y. Wang, X. Xing, F. Qiu, H. Liu, Y. Ma, D. Lin, T. Gao, *J. Biomater. Sci. Polym. Ed.* **2011**, *22*, 809.
- [8] A. Z. Ruiz, D. Bruehwiler, T. Ban, G. Calzaferri, *Monatsh. Chem.* **2005**, *136*, 77.
- [9] G. Calzaferri, K. Lutkouskaya, *Photochem. Photobiol. Sci.* **2008**, *7*, 879.
- [10] M. Tsotsalas, M. Busby, E. Gianolio, S. Aime, L. De Cola, *Chem. Mater.* **2008**, *20*, 5888.
- [11] a) N. S. Kehr, K. Riehemann, J. El-Gindi, A. Schaefer, H. Fuchs, H.-J. Galla, L. De Cola, *Adv. Funct. Mater.* **2010**, *20*, 2248; b) N. S. Kehr, A. Schaefer, B. J. Ravoo, L. De Cola, *Nanoscale* **2010**, *2*, 601.
- [12] R. Q. Albuquerque, J. Kuhni, P. Belsler, C. L. De, *ChemPhysChem* **2010**, *11*, 575.
- [13] L. D. White, C. P. Tripp, *J. Colloid Interface Sci.* **2000**, *232*, 400.
- [14] H. H. J. Persson, W. R. Caseri, U. W. Suter, *Langmuir* **2001**, *17*, 3643.
- [15] S. Onclin, A. Mulder, J. Huskens, B. J. Ravoo, D. N. Reinhoudt, *Langmuir* **2004**, *20*, 5460.
- [16] G. Calzaferri, N. Gfeller, *J. Phys. Chem.* **1992**, *96*, 3428.
- [17] S. Megelski, A. Lieb, M. Pauchard, A. Drechsler, S. Glaus, C. Debus, A. J. Meixner, G. Calzaferri, *J. Phys. Chem. B* **2001**, *105*, 25.
- [18] A. Mulder, S. Onclin, M. Peter, J. P. Hoogenboom, H. Beijleveld, M. J. ter, M. F. Garcia-Parajo, B. J. Ravoo, J. Huskens, H. N. F. van, D. N. Reinhoudt, *Small* **2005**, *1*, 242.
- [19] A. Mulder, T. Auletta, A. Sartori, S. Del Ciotto, A. Casnati, R. Ungaro, J. Huskens, D. N. Reinhoudt, *J. Am. Chem. Soc.* **2004**, *126*, 6627.
- [20] M. J. W. Ludden, A. Mulder, R. Tampe, D. N. Reinhoudt, J. Huskens, *Angew. Chem.* **2007**, *119*, 4182; *Angew. Chem. Int. Ed.* **2007**, *46*, 4104.
- [21] P. R. Ashton, R. Koeniger, J. F. Stoddart, D. Alker, V. D. Harding, *J. Org. Chem.* **1996**, *61*, 903.

Received: June 6, 2013

Revised: July 23, 2013

Published online: September 13, 2013